WILEY-VCH

Weilin Xu, Yuwei Zhang, and Tao Chen

Single Particle Nanocatalysis

Fundamentals and Applications

Single Particle Nanocatalysis

Single Particle Nanocatalysis

Fundamentals and Applications

Weilin Xu, Yuwei Zhang, and Tao Chen

WILEY-VCH

Authors

Prof. Weilin Xu
Changchun Institute of Applied Chemistry
5625 Renmin Street
130022 Changchun
China

Prof. Yuwei Zhang
Current affiliation:
Center for Advanced Analytical Science
c/o School of Chemistry and Chemical Engineering Guangzhou University
230 Wai Huan Xi Road, Guangzhou Higher Education Mega Center
510006 Guangzhou
China

Dr. Tao Chen
Current affiliation:
Universität Göttingen
Drittes Physikalisches Institut
Friedrich-Hund-Platz1
37077 Göttingen
Germany

Cover Image: © piranka/iStock.com

Library of Congress Card No.: applied for

British Library Cataloguing-in-Publication Data
A catalogue record for this book is available from the British Library.

Bibliographic information published by the Deutsche Nationalbibliothek
The Deutsche Nationalbibliothek lists this publication in the Deutsche Nationalbibliografie; detailed bibliographic data are available on the Internet at <http://dnb.d-nb.de>.

Print ISBN: 978-3-527-34329-4
ePDF ISBN: 978-3-527-80969-1
ePub ISBN: 978-3-527-80971-4
oBook ISBN: 978-3-527-80972-1

Cover Design Wiley
Typesetting SPi Global, Chennai, India
Printing and Binding

Printed on acid-free paper

10 9 8 7 6 5 4 3 2 1

Contents

Preface

Since the proposal of "nanocatalysis" in 1990s, all kinds of nanocatalysts have been extensively studied at ensemble level with all kinds of traditional methods. The main purpose of the study of "nanocatalysis" is to control the reaction rate and/or selectivity of some useful chemical reactions by varying the size, morphology, or surface chemical compositions of the nanomaterials with distinct and tunable chemical activity, specificity, and selectivity. About 10 years ago, the nanocatalysis was usually studied at ensemble level from the average of thousands of nanoparticles. Because of the heterogeneities of surface properties of nanoparticles, the knowledge about the structure–activity relationship of nanocatalysts obtained at ensemble level was usually not so precise.

In the last 10 years, with the achievement of detecting the weak electric or photonic signals, the nanocatalysis has been studied successfully at single molecule/single particle level to deeply address the heterogeneity challenge in nanocatalysis and reveal a more precise structure–activity relationship of nanocatalysts. In this book, we introduce and summarize the recent development of single molecule/particle nanocatalysis to provide both comprehensive coverage of fundamentals for different methods now in widespread use and the extensive applications in different catalytic systems. It is chaptered mainly based on different detection methods, including single molecule fluorescence microscopy, surface plasmon resonance spectroscopy, X-ray microscopy, and surface-enhanced Raman spectroscopy, etc., or their combinations.

This book is intended as a reference book not only for experts in this area but also for general researchers (such as graduate levels or interested individuals) who want to learn/realize how to study the nanocatalysis at single molecule/particle level. It includes numerous basic principles of different methods and application examples. Illustrations have been employed to clarify presentations, and the style is pedagogical to some extent. Knowledge of basic physical chemistry is assumed. The book emphasizes the mathematical theory underlying the methodology, so specialized mathematical background is needed; however, the key parts are their applications in different practical catalytic systems. The cited literature is extensive, ranging from early basic work to concrete experimental examples, including both research papers and reviews.

The book starts with an overview of the single molecule/particle catalysis by introducing concisely the history of some typical study methods for single molecule/particle nanocatalysis (Chapter 1), showing the origins of all kinds of

techniques for the detection of some weak signals. Then, there are individual discussions based on different detection tools. Firstly, the physical/mathematical basis of single molecule fluorescence microscopy (SMFM)-based catalytic kinetic and dynamic studies of individual nanoparticles and the applications of different catalytic models are introduced in detail (Chapter 2), the combination of such tool with other techniques, such as electrochemical techniques, and the atomic force microscopy (AFM), etc. (Chapter 3); moreover, as one of the key topics, the super-resolution imaging based on SMFM is also discussed in detail from its basic concept to its extensive application in some typical nanocatalytic systems (Chapter 4).

Next are discussions of other tools for single particle nanocatalysis study. The first one is scanning electrochemical microscopy (SECM) for single particle nanocatalysis, ranging from its history, principle, and applications in single particle nanocatalysis (Chapter 5), then the surface plasmon resonance spectroscopy for single particle nanocatalysis/reaction (Chapter 6), X-ray-based microscopy of single particle nanocatalysis (Chapter 7), vibrational spectroscopy (including the enhanced Raman spectroscopy/scattering and enhanced infrared spectroscopy) for single particle, and nanoscale catalysis (Chapter 8). At the end, some other not widely practiced techniques for single particle nanocatalysis/electrochemistry are also introduced (Chapter 9).

It should be noted that the list of abbreviations at the end of each chapter offers definitions. We have accommodated discussions of some techniques that are useful with detailed laboratory procedures, such as the experimental setup, included. Here, we owe thanks to many others who have helped with this project. We are especially grateful to Lifen Yang, Program Manager, Lesley Jebaraj, Project Editor, from Wiley. Without their assistance, this project will can never be proposed or done in time. We are grateful to Peng Chen from Cornell University, who led us to the field of single molecule nanocatalysis. We thank our many other colleagues throughout the single molecule community, who have given constructive comments and taught us patiently over the 2.5 years. At the end, we also thank our group members and families for affording us a large amount of time and freedom required to undertake this large project.

Weilin Xu
Yuwei Zhang
Tao Chen

1

The History/Development of Single Particle Nanocatalysis

Since the evolution of nanosciences at the end of the 1990s, the concept of "nanocatalysis" has come up with indicating the catalysis occurring on all kinds of nanomaterials or nanocatalysts. Ideally, these nanocatalysts should be able to speed up the wanted or slow down the unwanted chemical reactions with high efficiency, selectivity, and stability. Specific reactivity or utilization efficiency of the active components can be anticipated because of the unique tiny size in nanodimension that can afford specific properties that cannot be achieved with regular, bulk, or non-nanomaterials. In recent decades, nanocatalysis is one of the most exciting subfields of catalysis. Its central aim is to speed up some useful chemical reactions by varying the size, morphology, or surface chemical compositions of the nanomaterials with distinct and tunable chemical activity, specificity, and selectivity.

About 10 years ago, the nanocatalysis was usually studied at ensemble level. In this way, all the information obtained for nanocatalysis was from the average of thousands of nanoparticles. Therefore, the knowledge about the structure–activity relationship of nanocatalysts obtained at ensemble level was usually not so precise because of the fact that the surface properties of nanoparticles are intrinsically heterogeneous, owing to their structural dispersions, heterogeneous distribution of surface sites, and surface restructuring dynamics. This intrinsic heterogeneity can cause both nanoparticle-dependent and temporally varying catalytic properties. To address such heterogeneity challenge in nanocatalysis or reveal more precise structure–activity relationship of nanocatalysts, it is very desirable for us to study the catalytic process of nanocatalysts at the single-nanoparticle level in real time.

In the last decades, with the fast development of detection techniques for weak electric or photonic signals, the nanocatalysis study has been extended from bulk ensemble level to single molecule or single particle level via different detection methods, including electrochemical methods, single molecule fluorescence microscopy, surface plasmon resonance (SPR) spectroscopy, X-ray microscopy, and surface-enhanced Raman spectroscopy, etc., or their combination. It has been known that single molecule or single particle measurements of nanocatalysis can reveal the catalytic properties of individual particles or molecules and then obtain distribution of catalytic properties of nanoparticles in inhomogeneous systems. The distributions, which can be either static or

Single Particle Nanocatalysis: Fundamentals and Applications,
First Edition. Weilin Xu, Yuwei Zhang, and Tao Chen.

dynamical, usually cannot be revealed by ensemble-averaged measurements. Such new information usually can further improve our understanding to the surface nanocatalysis process. In the following, the history of some typical study methods for single particle nanocatalysis is introduced concisely.

1.1 History of Single Particle Nanocatalysis Based on Single Molecule Fluorescence Microscopy

The single molecule fluorescence microscopy was initially developed for the study of biological systems, such as single enzymes, cells, or other types of single biological macromolecules. In the early time, the traditional fluorescence microscope uses fluorescence signals from samples, such as large biological objects (such as cells and neurons), to generate an image with low spatial resolution ($\sim\lambda/2$, λ is the wavelength of photons) limited by the optical diffraction and the sensitivity of photon detectors. With the development of science and technologies for photon detection, after 1940s, based on different mechanisms, many types of photodetectors were invented to detect individual photons, including photomultipliers, Geiger counters, single-photon avalanche diodes, superconducting nanowire single-photon detectors, transition edge sensors, or scintillation counters, etc. Single-photon detection is useful in many fields including fiber optic communication, quantum information science, quantum encryption, medical imaging, light detection and ranging, DNA sequencing, astrophysics, and materials science. Especially with the development of charge-coupled devices (CCDs, 1969), the fluorescence of single molecule could be detected via electron-multiplying (EM) CCD camera cheaply.

For the typical application of single molecule fluorescence microscopy in biology, in 1998, Sunny Xie and coworker studied the single molecule enzymatic dynamics of single cholesterol oxidase molecules by real-time monitoring the emission from the enzyme's fluorescent active site [1]. In this work, for the first time, statistical analyses of single molecule trajectories were adopted to reveal the reaction rate fluctuation, the molecular memory effect, and the static and dynamic disorder of reaction rates at single molecule level, which are essentially indistinguishable in ensemble-averaged experiments. This pioneering work exemplified explicitly the advantages of single molecule methods over traditional ensemble approaches. After that, such method has been applied extensively to study many other biological systems at single particle (or molecule) level [2].

The first single particle nanocatalysis with the above-mentioned single molecule fluorescence microscopy was done in 2006 [3]. In this work, by counting the single turnovers on catalysts of individual large (>10 um) layered double hydroxide (LDH) particles, the crystal-face-dependent catalytic activity was spatially resolved half-quantitatively without detailed kinetic analysis. The first catalytic kinetic and dynamic study of single nanoparticles was done two years later by Peng Chen and coworkers [4, 5]. In this work, a Langmuir–Hinshelwood mechanism for the catalytic kinetic study of a single particle was proposed for

the first time. Such mechanism is applicable for the product formation and dissociation processes on individual nanoparticles or enzyme molecules with the number of active sites larger than 1; based on such mechanism, with the same single particle approach with single-turnover resolution under single molecule fluorescence microscopy, they studied the redox catalysis of individual colloidal Au nanoparticles in about 5 nm. It was revealed for the first time that the product formation process on individual Au nanoparticles indeed follow the Langmuir–Hinshelwood mechanism but with heterogeneous catalytic activity probably because of the size difference among different individual nanoparticles; as for the product dissociation process, three different dissociation behaviors were revealed to exist in these nanoparticles; also, the indirect or substrate-associated dissociation pathway of product molecules and the spontaneous- and catalysis-induced dynamic surface restructuring of individual Au nanoparticles were revealed for the first time. Such new information undistinguishable from ensemble experiments exemplified the power of the single particle method in the modern surface nanocatalysis.

After this work, the catalytic kinetics of some other nanocatalytic systems (such as Pt, Au, Pd, and TiO_2) were also studied similarly with such method and mechanisms at single particle level [6–10].

Besides the catalytic kinetics of nanocatalysts at single particle level, the catalytic thermal properties of individual nanocatalysts could also be studied at single particle level based on a temperature-controllable single molecule fluorescence microscopy [11].

On the other hand, tremendous efforts have also made to improve the spatial resolution of such optical microscopy. Because of a diffraction limitation, the spatial resolution of a conventional optical microscopy is only about 200 nm for visible light. To visualize and then study the nanoscale properties reliably, early researchers made great efforts to break the optical diffraction limit by bringing the resolution of optical microscopy down to few nanometers [12]. Such breakthrough expedited a new technique of super-resolution (SR) fluorescence microscopy, through which many nanoscale structure or dynamics now can be visualized and then investigated directly. Recently, such technique has been extended successfully from biological areas to heterogeneous nanocatalysis [13–18].

1.2 History of Single Particle Nanocatalysis Based on (Localized) Surface Plasmon Resonance

SPR is the resonant oscillation of conduction electrons at the interface between two types of materials with different refractive indices, stimulated by incident light. Or, simply, it is a physical process that can occur when plane-polarized light hits a thin metal film under total internal reflection conditions. SPR is the basis of many standard tools for measuring adsorption of material onto planar metal (typically gold or silver) surfaces or onto the surface of metal nanoparticles. Its first use in a real-time analysis of a biological system was in 1990s, after that, as

a label-free optical method, the SPR has become a popular optical sensing technology in many kinds of biological and medical areas because of its real-time and noninvasive nature.

For nanoparticles, in the early time, the SPR signal was usually adopted to study the shape- or size-dependent variation of radiative, nonradiative and photothermal properties of nanoparticles at ensemble level [19]. The first SPR-based single particle catalysis was done in 2010 [20]. In this work, Tao and coworkers introduced a strategy to image the electrocatalytic current of single nanoparticles by sensing local electrochemical current via SPR. Such technique possesses high spatial resolution and sensitivity because the signal varies with current density rather than current. The imaging technique is noninvasive, scanning-free, and fast, making it a powerful tool for studying heterogeneous surface reactions and for analyzing trace chemicals. Based on the strategy mentioned above, recently, this method was further used to study the electrocatalytic reaction of individual Pt nanoparticles by observing the decrease of the refractive index or the variation of SPR signal near the electrode surface because of the formation of hydrogen reduction process [21].

Furthermore, the localized surface plasmon resonance (LSPR) is the plasmon oscillating locally around a particle with diameter much smaller than the wavelength of incident light. The LSPR is also sensitive to the changes of surroundings of a nanoparticle, which make LSPR being an ideal tool to sense chemical reactions around or on a single particle, including its catalysis. Similar to SPR, the LSPR was also widely used in biological and biomedical sensing. In recent two decades, the LSPR was applied to study the various chemical reactions, such as electrochemical reaction, heterogeneous catalysis, and photocatalysis. Many kinds of LSPR-based strategies were developed based on the catalytic systems at single particle level. However, most of these studies are at the stage of sensing reactions and not deep yet to the explanation of catalytic mechanism.

1.3 History of Single Particle Nanocatalysis Based on Scanning Electrochemical Microscopy

Scanning electrochemical microscopy (SECM) based on an ultra-microelectrode (UME) was invented by Allen J. Bard et al. [22]. SECM can be used to study the local electrochemical behaviors of liquid/solid, liquid/gas, and liquid/liquid interfaces by measuring the diffusion-limited current at a UME tip as a function of precise tip position over a substrate region of interest. Two-dimensional raster scan of the UME can generate images of surface reactivities of all kinds of materials, such as electrocatalyst materials, enzymes, and other biological systems [23].

In 1997, Bard and coworker observed the single electron transfer events at a nanometer electrode, indicating a single molecule resolution achieved on UME [24]. Later on, many efforts have been made to prepare UMEs with all kinds of methods, including the transfer or deposition of single metal nanoparticles to/on the tips of UMEs [25]. After that, very few studies have been done for

the real single particle nanocatalysis with SECM as most of the relevant studies are actually about the collisions of single nanoparticles on UMEs by monitoring the current generated through the single-particle-catalyzed reactions [26]. The first study of single particle nanocatalysis based on SECM was done by Stimming and coworkers in 2003. In this work, they studied the catalytic reactivity of supported single Pd nanoparticles for hydrogen evolution reaction using an electrochemical scanning tunneling microscopy (STM) setup [27]. Later on, in 2005, based on rapid-imaging mode, SECM was adopted to screen rapidly the arrays of bimetal electrocatalysts with compositions in a wide range for high efficient oxygen reduction reaction [28].

In recent years, the SECM technique was mainly used extensively in the field of analytical chemistry, while very rare for single particle nanocatalysis.

1.4 History of Single Particle Nanocatalysis Based on Vibrational Spectroscopies

Vibrational spectroscopies, including Raman spectroscopy and infrared (IR) spectroscopy, have been the most common technique to identify the components and structures of samples. However, because of the low Raman scattering and infrared adsorption cross sections of molecules, the studies of normal vibrational spectroscopy are limited in ensemble level. The discovery of surface-specific signal enhancement by plasmonic material led to a fast development of vibrational spectroscopy. The high sensitivity of them even enables single molecule detection at single particle level.

The phenomenon of Raman scattering was discovered in 1928 [29], whereas the first observation of enhanced Raman scattering (ERS) was in 1973 [30] and single molecule ERS in 1977 [31, 32]. It was realized that the tremendous enhancement of Raman signal can somehow rival the fluorescence signal. The application of ERS in single particle catalysts is still very rare mainly due to the usually low enhancement factors from a single particle, the small number of detected molecules, and the high requirement for instrument. Some early representative work was mainly about the studying or monitoring of catalysis on a single particle or at the nanoscale via ERS technique [33].

On the other hand, the technique of surface-enhanced infrared adsorption spectroscopy (SEIRAS) was commercialized in the early 1980s [34]. It allows sub-monolayer detection of molecules absorbed at a surface. Based on it, in the last year (2017), Wu et al. used the synchrotron-radiation-based infrared nanospectroscopy to map the surface catalytic activity of individual particles with high spatial resolution [35]. It is the first case or the only case reported by now with IR for the study of single particle nanocatalysis.

Even though, with the fast development of science and technologies, it can be expected that the techniques based on vibrational spectroscopies will be applied widely in more single particle catalysis because of their advantages of revealing the structural information of molecules.

References

1 Lu, H.P. and Xie, X.S. (1998). Single-molecule spectral fluctuations at room temperature. *Nature* 385: 143–146.

2 Smiley, R.D. and Hammes, G.G. (2006). Single molecule studies of enzyme mechanisms. *Chemical Reviews* 106: 3080–3094.

3 Roeffaers, M.B., Sels, B.F., Uji-i, H. et al. (2006). Spatially resolved observation of crystal-face-dependent catalysis by single turnover counting. *Nature* 439: 572–575.

4 Xu, W., Kong, J.S., Yeh, Y.-T.E., and Chen, P. (2008). Single-molecule nanocatalysis reveals heterogeneous reaction pathways and catalytic dynamics. *Nature Materials* 7: 992–996.

5 Xu, W., Kong, J.S., and Chen, P. (2009). Single-molecule kinetic theory of heterogeneous and enzyme catalysis. *Journal of Physical Chemistry C* 113: 2393–2404.

6 Tachikawa, T., Wang, N., Yamashita, S. et al. (2010). Design of a highly sensitive fluorescent probe for interfacial electron transfer on a TiO_2 surface. *Angewandte Chemie International Edition* 49: 8593–8597.

7 Tachikawa, T., Yamashita, S., and Majima, T. (2011). Evidence for crystal-face-dependent TiO_2 photocatalysis from single-molecule imaging and kinetic analysis. *Journal of the American Chemical Society* 133: 7197–7204.

8 Chen, T., Chen, S., Zhang, Y. et al. (2016). Catalytic kinetics of different types of surface atoms on shaped Pd nanocrystals. *Angewandte Chemie International Edition* 55 (5): 1839–1843.

9 Chen, T., Zhang, Y., and Xu, W. (2016). Size-dependent catalytic kinetics and dynamics of Pd nanocubes: a single-particle study. *Physical Chemistry Chemical Physics* 18: 22494–22502.

10 Han, K.S., Liu, G., Zhou, X. et al. (2012). How does a single Pt nanocatalyst behave in two different reactions? A single-molecule study. *Nano Letters* 12 (3): 1253–1259.

11 Chen, T., Zhang, Y., and Xu, W. (2016). Single-molecule Nanocatalysis reveals catalytic activation energy of single nanocatalysts. *Journal of the American Chemical Society* 138: 12414–12421.

12 Basche, T., Moerner, W.E., Orrit, M., and Wild, U.P. *Single-Molecule Optical Detection, Imaging and Spectroscopy*. Weinheim: Wiley-VCH.

13 Cremer, G.D., Sels, B.F., Vos, D.E.D. et al. (2015). NASCA microscopy: super-resolution mapping of chemical reaction centers. In: *Far-Field Optical Nanoscopy* (ed. P. Tinnefeld, C. Eggeling and W.S. Hell), 245–261. Berlin, Heidelberg: Springer.

14 Habuchi, S. (2014). Super-resolution molecular and functional imaging of nanoscale architectures in life and materials science. *Frontiers in Bioengineering and Biotechnology* 2: 20.

15 Wang, W., Gu, J., He, T. et al. (2015). Optical super-resolution microscopy and its applications in nano-catalysis. *Nano Research* 8 (2): 441–455.

16 Whelan, D.R. and Bell, T.D.M. (2015). Super-resolution single-molecule localization microscopy: tricks of the trade. *Journal of Physical Chemistry Letters* 6 (3): 374–382.
17 Janssen, K.P.F., De Cremer, G., Neely, R.K. et al. (2013). Single molecule methods for the study of catalysis: from enzymes to heterogeneous catalysts. *Chemical Society Reviews* 43: 990–1006.
18 Chen, P., Zhou, X., Andoy, N.M. et al. (2013). Spatiotemporal catalytic dynamics within single nanocatalysts revealed by single-molecule microscopy. *Chemical Society Reviews* 43: 1107–1117.
19 Link, S. and El-Sayed, M.A. (2000). Shape and size dependence of radiative, non-radiative and photothermal properties of gold nanocrystals. *International Reviews in Physical Chemistry* 19: 409–453.
20 Shan, X., Patel, U., Wang, S. et al. (2010). Imaging local electrochemical current via surface plasmon resonance. *Science* 327: 1363–1366.
21 Shan, X., Díez-Pérez, I., Wang, L. et al. (2012). Imaging the electrocatalytic activity of single nanoparticles. *Nature Nanotechnology* 7: 668–672.
22 Bard, A.J., Fan, F.R.F., Kwak, J., and Lev, O. (1989). Scanning electrochemical microscopy. Introduction and principles. *Analytical Chemistry* 61: 132–138.
23 Bard, A.J., Denuault, G., Lee, C. et al. (1990). Scanning electrochemical microscopy – a new technique for the characterization and modification of surfaces. *Accounts of Chemical Research* 23 (11): 357–363.
24 Fan, F.-R.F. and Bard, A.J. (1997). Am electrochemical coulomb staircase: detection of single electron-transfer events at nanometer electrodes. *Science* 277: 1791–1793.
25 Chen, S. and Kucernak, A. (2003). Electrodeposition of platinum on nanometer-sized carbon electrodes. *Journal of Physical Chemistry B* 107: 8392–8402.
26 Xiao, X. and Bard, A.J. (2007). Observing single nanoparticle collisions at an ultramicroelectrode by electrocatalytic amplification. *Journal of the American Chemical Society* 129: 9610–9612.
27 Meier, J., Friedrich, K.A., and Stimming, U. (2002). Novel method for the investigation of single nanoparticle reactivity. *Faraday Discussions* 121: 365–372.
28 Fernandez, J., Walsh, D.A., and Bard, A.J. (2005). Thermodynamic guidelines for the design of bimetallic catalysts for oxygen electroreduction and rapid screening by scanning electrochemical microscopy. M–Co (M: Pd, Ag, Au). *Journal of the American Chemical Society* 127: 357–365.
29 Raman, C. and Krishnan, K. (1928). A new type of secondary radiation. *Nature* 121: 501.
30 Fleischmann, M., Hendra, P.J., and McQuillan, A.J. (1974). Raman spectra of pyridine adsorbed at a silver electrode. *Chemical Physics Letters* 26 (2): 163–166.
31 Nie, S. and Emory, S.R. (1997). Probing single molecules and single nanoparticles by surface-enhanced Raman scattering. *Science* 275 (5303): 1102–1106.
32 Kneipp, K., Wang, Y., Kneipp, H. et al. (1997). Single molecule detection using surface-enhanced Raman scattering (SERS). *Physical Review Letters* 78 (9): 1667–1670.

33 Kumar, N., Stephanidis, B., Zenobi, R. et al. (2015). Nanoscale mapping of catalytic activity using tip-enhanced Raman spectroscopy. *Nanoscale* 7 (16): 7133–7137.

34 Hartstein, A., Kirtley, J.R., and Tsang, J.C. (1980). Enhancement of the infrared absorption from molecular monolayers with thin metal Overlayers. *Physical Review Letters* 45 (3): 201–204.

35 Wu, C.-Y., Wolf, W.J., Levartovsky, Y. et al. (2017). High-spatial-resolution mapping of catalytic reactions on single particles. *Nature* 541 (7638): 511–515.

2

Single Molecule Nanocatalysis Reveals Catalytic Kinetics and Thermodynamics of Individual Nanocatalysts

In this chapter, the single molecule fluorescence microscopy (SMFM)-based study of catalytic kinetics and thermodynamics of individual nanocatalysts are introduced in detail. For a better understanding of the development history of SMFM-based kinetic study of all kinds of catalysis, all the contents in this chapter will be organized in the time order based on the date for their first arising. Therefore, as the base, the single molecule enzymology will be introduced first.

2.1 Single Molecule Enzymology

Enzymes can high efficiently catalyze biochemical reactions. To understand how an enzyme works as a biological catalyst at the molecular level, in 1990s, based on photon-sensitive tools, SMFM was quickly adopted extensively in this field [1, 2]. For single molecule (SM) enzymology, one of the pioneering researchers is Sunney Xie from Harvard University [3–11]. In early 1990s, Xie and coworkers developed the technique of single molecule imaging and spectroscopy based on fluorescence signal from single molecules. The extensive application of the technique has led to the formation of a hot research field by addressing many compelling problems in biology at single molecule level. The *in vitro* study of single molecule enzymology has brought some deep understanding of the mechanism and fundamental insights into enzymatic catalysis. In 1998, Xie et al. made the first real-time observation of enzymatic turnovers of a single flavoenzyme by monitoring the redox-induced fluorescence variation of the individual enzymes [3]. Later on, they found that the Michaelis–Menten equation, more than 100 years old, holds even at single molecule level [10, 11].

2.1.1 Single Molecule Michaelis–Menten Kinetics in the Absence of Dynamic Disorder

This section mainly summarizes the theoretical understanding of the single molecule Michaelis–Menten mechanism or kinetics of enzymes [10]. Single molecule experiments based on SMFM can measure the probability density $f(t)$ of the stochastic waiting time t for individual turnover events. $f(t)$ is related with ensemble kinetic parameters, but the information obtained from it is much more

Single Particle Nanocatalysis: Fundamentals and Applications,
First Edition. Weilin Xu, Yuwei Zhang, and Tao Chen.

than that obtained from ensemble results; particularly, the dynamic disorder or activity fluctuation due to the reconstruction of enzymes, which can never be probed by traditional ensemble measurement, can be revealed explicitly via such a single molecule method. In the following, the deduction of the single molecule Michaelis–Menten equation will be presented in detail.

For comparison, the classic Michaelis–Menten mechanism for the ensemble catalytic activity of enzymes is introduced first below: a substrate (S) molecule can bind reversibly with an enzyme (E) molecule to form a complex of ES that decomposes quickly to release a free product (P) molecule and regenerate the free E for next catalytic cycle via the following equation:

$$E + S \underset{k_{-1}}{\overset{k_1}{\rightleftarrows}} ES \xrightarrow{k_2} E^0 + P, \quad E^0 \xrightarrow{\delta} E \tag{2.1}$$

The product formation rate v for the above Michaelis–Menten mechanism can be deduced as follows:

$$v = k_2[E]_T \frac{[S]}{([S] + K_M)} = v_{max} \frac{[S]}{([S] + K_M)} \tag{2.2}$$

where $[E]_T$ is the total enzyme concentration in the reactor, $K_M = (k_{-1} + k_2)/k_1$, and $v_{max} = k_2[E]_T$. This is the classic rate expression for the ensemble-averaged enzyme kinetics.

According to Eq. (2.1), with t as the elapsed time from the onset of an experiment, the rate equations in the first step can then be expressed as

$$\frac{d[E]}{dt} = -k_1[E][S] + k_{-1}[ES] \tag{2.3}$$

$$\frac{d[ES]}{dt} = k_1[E][S] - (k_{-1} + k_2)[ES] \tag{2.4}$$

$$\frac{d[E^0]}{dt} = \frac{d[P]}{dt} = k_2[ES] \tag{2.5}$$

The initial (at $t = 0$) conditions for these equations are $[E^0] = 0$ and $[ES] = 0$. At early time, only very few S molecules can be converted to P; then, the second step in Eq. (2.1) can be neglected. In order to solve the above nonlinear differential Eqs. (2.3)–(2.5) exactly, it is assumed that the concentration of intermediate ES can reach a steady state ($d[ES]/dt = 0$) in short time after the onset of the reaction. Based on such steady-state approximation, with $[E]_T = [E] + [ES]$, Eqs. (2.3)–(2.5) are easily solved to obtain the classic Michaelis–Menten equation:

$$v = \frac{v_{max}[S]}{[S] + K_M} \tag{2.6}$$

where v_{max} is the maximum reaction rate ($=k_2[E]_T$) at saturating substrate concentration and K_M ($=(k_{-1}+k_2)/k_1$) is the Michaelis constant and equals to the substrate concentration ($[S]$) at which the enzymatic rate is half of the v_{max}.

In a single molecule experiment, the fluorescence of a single-enzyme molecule E is monitored continuously as it goes back and forth repetitively through the states E, ES, and E^0 as shown in Eq. (2.1). In this case, the waiting time to complete

the first reaction, a stochastic variable, can be described explicitly by a waiting time distribution via probability density $f(t)$. To obtain the kinetic equations for the single molecule Michaelis–Menten mechanism, the concentrations of all species in Eqs. (2.3)–(2.5) are replaced by the probabilities (P) of the E molecule in the forms of E, ES, and E^0:

$$\frac{dP_E(t)}{dt} = -k_1^0 P_E(t) + k_{-1} P_{ES}(t) \tag{2.7}$$

$$\frac{dP_{ES}(t)}{dt} = k_1^0 P_E(t) - (k_{-1} + k_2) P_{ES}(t) \tag{2.8}$$

$$\frac{dP_{E^0}(t)}{dt} = k_2 P_{ES}(t) \tag{2.9}$$

with the initial (at $t = 0$) conditions $P_E(0) = 1$, $P_{ES}(0) = 0$, and $P_{E^0}(0) = 0$ and the constraint of $PE(t) + P_{ES}(t) + P_{E^0}(t) = 1$ at any time. As the substrate depletion by a single-enzyme molecule is negligible, then $[S]$ could be regarded as a constant, and the rate constant $k_1^0 (= k_1[S])$ for the forward step in Eq. (2.1) could be taken as a pseudo-first-order rate constant in approximation. The conversion from E^0 to E can occur either instantaneously [12] or through a ping-pong mechanism based on some other fast reactions [3].

Obviously, $P_E(t)$, $P_{ES}(t)$, and $P_{E^0}(t)$ can be obtained by solving the linear first-order differential Eqs. (2.7)–(2.9). With known $P_{E^0}(t)$, the waiting time distribution or the probability density $f(t)$ can be further obtained with constraint $\int_0^\infty dt f(t) = 1$: The probability for a turnover to occur between the time t and $t + \Delta t$ equals $f(t)\Delta t$; $f(t)\Delta t$ also equals the probability ($\Delta P_{E^0}(t)$) for the enzyme in state E^0 in the interval between t and $t + \Delta t$, then $\Delta P_{E^0}(t) = k_2 P_{ES}(t)\Delta t$. Therefore, with Δt infinitesimal, one can obtain

$$f(t) = \frac{dP_{E^0}(t)}{dt} = k_2 P_{ES}(t) \tag{2.10}$$

From the solutions of Eqs. (2.7)–(2.9), $f(t)$ shown in Eq. (2.10) can be easily obtained:

$$f(t) = \frac{k_1 k_2 [S]}{2A} [\exp(A + B)t - \exp(B - A)t] \tag{2.11}$$

where $A = \sqrt{(k_1[S] + k_{-1} + k_2)^2/4 - k_1 k_2 [S]}$ and $B = -(k_1[S] + k_{-1} + k_2)/2$.

Figure 2.1 shows the time (t) dependence of $f(t)$ at different values of parameters: (i) top panel with $k_{-1} = 0$, no backward reaction from ES to E and S, (ii) middle panel with $k_{-1} = 50\ s^{-1}$, the catalytic rate and backward dissociation rate are comparable, and (iii) bottom panel with $k_{-1} = 2000\ s^{-1}$, the backward dissociation rate from ES to E and S is much larger than the catalytic rate.

At the limit $k_{-1} \to 0$ (top panel shown in Figure 2.1), the catalytic reaction can be described with the sequential reaction: $S + E \xrightarrow{k_1^0} ES \xrightarrow{k_2} E_0 + P$. The corresponding waiting time distribution or the probability density $f(t)$ is the convolution of $f_1(t)$ and $f_2(t)$ for the two sequential steps, i.e. $f(t) = \int_0^t dt' f_1(t - t') f_2(t')$. If $f_1(t) = k_1[S] \exp(-k_1[S]t)$ and $f_2(t) = k_2[S] \exp(-k_2 t)$, then $f(t)$ is

$$f(t) = \frac{k_1 k_2 [S]}{k_2 - k_1 [S]} [\exp(-k_1[S]t) - \exp(-k_2 t)] \tag{2.12}$$

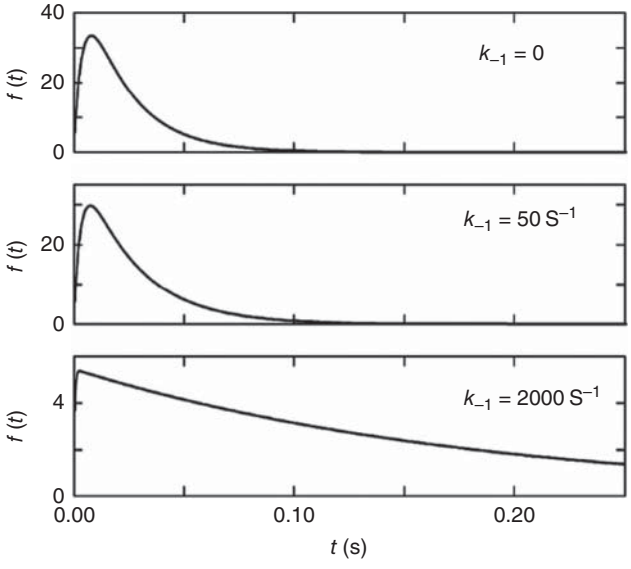

Figure 2.1 Probability density of the waiting time, $f(t)$, in the absence of dynamic disorder, as calculated from Eq. (2.11), for three different values of k_{-1} (0, 50, and 2000 s^{-1}) with $k_1 = 107\ M^{-1}\ s^{-1}$, $k_2 = 250\ s^{-1}$, and $[S] = 0.005$ mM. Source: Reprinted with permission from Kou et al. [10]. Copyright 2005, ACS.

Obviously, such $f(t)$ rises exponentially first and then decays exponentially, corresponding to the ES generation (large k_1 and k_2) and decomposition (small k_1 and k_2).

As shown in the bottom panel of Figure 2.1, when the decomposition of ES is very fast, $f(t)$ is a simple single-exponential decay function. Then, the reaction reaches a special steady-state limit in which $[ES]$ is almost a constant: $dP_{ES}(t)/dt = 0$ when $k_2 \ll k_{-1}$. Along with the initial condition $P_{E0}(0) = 0$ and the constraint $P_E(t) + P_{ES}(t) + P_{E0}(t) = 1$, the $dP_{ES}(t)/dt = 0$ can lead to

$$P_{E^0}(t) = 1 - \exp\left(-\frac{k_1^0 k_2 t}{k_1^0 + k_{-1} + k_2}\right) \tag{2.13}$$

Along with Eq. (2.10), one can further obtain

$$f(t) = \frac{k_1 k_2 [S]}{k_1[S] + k_{-1} + k_2} \exp\left(-\frac{k_1 k_2 [S] t}{k_1[S] + k_{-1} + k_2}\right) \tag{2.14}$$

consistent with the single-exponential decay shown in the bottom panel of Figure 2.1. When $[S] \to \infty$, as expected, $f(t)$ can be further reduced to a simpler form ($=k_2 \exp(-k_2 t)$).

Furthermore, the mean waiting time ($\langle t \rangle$) for the reaction could be obtained: $\langle t \rangle = \int_0^\infty dt\, t f(t)$, which is also the first moment of $f(t)$. It gives the connection of single molecule methods with traditional ensemble measurements as the reciprocal of $\langle t \rangle (\langle t \rangle^{-1})$ can be taken as an ensemble-averaged reaction rate [13]. Such connection could be generally attributed to the equivalence between time averaging and ensemble averaging. Moreover, the following results can be deduced

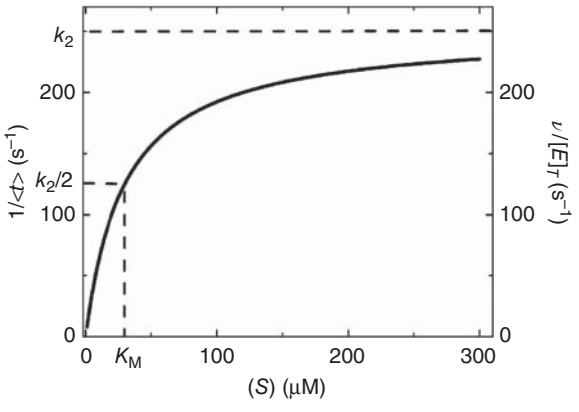

Figure 2.2 Average reaction rate $1/\langle t \rangle$ or its equivalent $v/[E]_T$, as calculated from Eq. (2.15), the single molecule Michaelis–Menten equation, as a function of substrate concentration [*S*] for $K_M = 30$ μM (the value corresponding to $k_{-1} = 50\ s^{-1}$, $k_2 = 250\ s^{-1}$, and $k_1 = 10^7\ M^{-1}\ s^{-1}$). Source: Reprinted with permission from Kou et al. [10]. Copyright 2005, ACS.

from Eq. (2.11):

$$\frac{1}{\langle t \rangle} = -\frac{(A^2 - B^2)^2}{2Bk_1k_2[S]} = \frac{k_2[S]}{[S] + K_M} \tag{2.15}$$

A comparison between Eqs. (2.6) and (2.15) indicates that $v/[E]_T = 1/\langle t \rangle$ or that $v/v_{max} = 1/(k_2\langle t \rangle)$.

Interestingly, the above results indicate that the classic Michaelis–Menten equation can be recovered from the first moment of $f(t)$, no matter whether the steady-state approximation is adopted or not in the calculations of single molecule probability, so Eq. (2.15) is named as single molecule Michaelis–Menten equation.

The [*S*] dependence of $1/\langle t \rangle$ with the parameters adopted in Figure 2.1 (the middle panel) is plotted in Figure 2.2. As expected, it exhibits the same characteristic hyperbolic profile as that for the classic Michaelis–Menten saturation curve. Such fact further confirms the consistency between the ensemble-averaged and single molecule kinetics. However, it should be noted that $f(t)$ indeed can provide more information than the ensemble method as the first moment is not the only information that can be obtained from $f(t)$, especially in the presence of dynamic disorder as discussed later on.

2.1.2 Single Molecule Michaelis–Menten Kinetics with Dynamic Disorder

It has been known that the waiting time distribution for some enzyme systems [14] can show multiexponentiality, which is different from $f(t)$ derived in Section 2.1.1. Such difference can be caused by the existence of dynamic disorder in real enzyme systems. To model the dynamic disorder of an enzyme system, the relevant parameters (such as k_2) can be assumed as stochastic variables that can fluctuate according to some prescribed statistics [15, 16]. The following section will establish the general Michaelis–Menten equation for the system with dynamic disorder to explain the concentration-dependent multiexponentiality of $f(t)$ observed in single molecule kinetic study.

(i) *Two-state model*: Firstly, the Michaelis–Menten mechanism was extended by simply incorporating the dynamic disorder. In this kinetic scheme, the enzyme in different states, E, ES, and E^0, can interconvert between two different conformations:

$$\begin{array}{l} S + E_1 \underset{k_{-11}}{\overset{k_{11}[s]}{\rightleftarrows}} ES_1 \overset{k_{21}}{\rightarrow} P + E_1^0 \overset{\delta_1}{\rightarrow} E_1 \\ \alpha \uparrow\downarrow \alpha \quad \beta \uparrow\downarrow \beta \quad \gamma \uparrow\downarrow \gamma \\ S + E_2 \underset{k_{-12}}{\overset{k_{12}[s]}{\rightleftarrows}} ES_2 \overset{k_{22}}{\rightarrow} P + E_2^0 \overset{\delta_2}{\rightarrow} E_2 \end{array} \tag{2.16}$$

However, one can see that the calculation of $f(t)$ and its first moment from Eq. (2.16) is still theoretically challenging. In such case, each new reaction cycle begins from either E_1 or E_2 with probabilities reflecting the steady-state populations of all kinds of intermediates. Therefore, the weighted average should be considered for the calculation of the total $f(t)$:

$$f(t) = w_1 f_{T_{E_1}}(t) + w_2 f_{T_{E_2}}(t) \tag{2.17}$$

where $f_{T_{E_1}}(t)$ and $f_{T_{E_2}}(t)$ are the distributions of the waiting times T_{E1} and T_{E2} or probability densities for enzyme (E) to complete the reaction starting from E_1 and E_2, respectively, and w_1 and w_2 are the corresponding steady-state probabilities for the enzyme E to stay in one or the other of these two conformations. The w_1 and w_2 can be deduced from the master equation formalism used to derive Eqs. (2.7)–(2.9), whereas the $f(t)$ calculation requires a different approach and can be found only in closed form in the Laplace domain. Based on the above equation, the final Laplace transform of $f(t)$ could be obtained:

$$\widetilde{f}(s) = (W_1, W_2, 0, 0)\widetilde{\mathbf{f}}(s) \tag{2.18}$$

where $\widetilde{f}(s)$ is the Laplace transform of $f(t)$ and $\widetilde{\mathbf{f}}(s) \equiv (\widetilde{f}_{T_{E_1}}(s), \widetilde{f}_{T_{E_2}}(s), \widetilde{f}_{T_{ES_1}}(s), \widetilde{f}_{T_{ES_2}}(s))^T$ is defined by

$$\widetilde{\mathbf{f}}(s) = (s\mathbf{I} - \mathbf{Q})^{-1}\mathbf{r} \tag{2.19}$$

where $\mathbf{I}$ is the identity matrix, $\mathbf{r} \equiv (0, 0, k_{21}, k_{22})^T$, and

$$\mathbf{Q} = \begin{pmatrix} -(\alpha + k_{11}[S]) & \alpha & k_{11}[S] & 0 \\ \alpha & -(\alpha + k_{12}[S]) & 0 & k_{12}[S] \\ k_{-11} & 0 & -(\beta + k_{-11} + k_{21}) & \beta \\ 0 & k_{-12} & \beta & -(\beta + k_{-12} + k_{22}) \end{pmatrix} \tag{2.20}$$

With the fast reset of $E_1{}^0$ and $E_2{}^0$ to E_1 and E_2 and the condition $\delta_1, \delta_2 \gg 1$, w_1 and w_2 satisfy

$$w_1 + w_2 = 1 \tag{2.21}$$

From these conditions, one can obtain

$$\frac{W_1}{W_2} = \frac{k_{21}[\,\alpha(k_{11}k_{22} + k_{11}k_{-12}) + \alpha\beta(k_{11} + k_{12}) + \beta k_{11}k_{12}[S]}{k_{22}[\,\alpha(k_{12}k_{21} + k_{12}k_{-11}) + \alpha\beta(k_{11} + k_{12}) + \beta k_{11}k_{12}[S]} \tag{2.22}$$

The complete solution in Laplace space to the waiting time distribution of the two-state model can be obtained from Eqs. (2.17)–(2.22). The first moment ($\langle t\rangle$) of $f(t)$ can be obtained easily from the formula: $\langle t\rangle = -\,\mathrm{d}\widetilde{f}(s)/\mathrm{d}s|_{s=0}$. From it, one can obtain that

$$\frac{1}{\langle t\rangle} = \frac{F^{-1}[S]}{[\mathrm{S}] + \frac{G[\mathrm{S}]+H}{FJ[\mathrm{S}]+FK}} \tag{2.23}$$

where the constants F, G, H, and K are given by

$$F = \frac{2}{k_{21} + k_{22}} \tag{2.24a}$$

$$G = \alpha(k_{21} - k_{22})\frac{k_{12}(k_{21} + k_{-11}) - k_{11}(k_{22} + k_{-12})}{k_{21} + k_{22}} + \beta[k_{12}(k_{21} + k_{-11}) + k_{11}(k_{22} + k_{-12})] \tag{2.24b}$$

$$H = 2\alpha(k_{22} + k_{-12})(k_{21} + k_{-11}) + 2\alpha\beta(k_{21} + k_{22} + k_{-11} + k_{-12}) \tag{2.24c}$$

$$J = \beta k_{11}k_{12}(k_{21} + k_{22}) \tag{2.24d}$$

$$K = \alpha[k_{11}k_{21}(k_{22} + k_{-12}) + k_{12}k_{22}(k_{21} + k_{-11})] + \alpha\beta(k_{11} + k_{12})(k_{21} + k_{22}) \tag{2.24e}$$

Here, $1/\langle t\rangle$ is the ensemble-averaged rate (by the assumption of ergodicity). Eq. (2.23) indicates that the rate of $1/\langle t\rangle$ does not always obey the Michaelis–Menten mechanism. However, under some limiting conditions, it does produce the hyperbolic relationship like that shown by Michaelis–Menten equation: (i) $k_{21} \gg \beta$, $k_{22} \gg \beta$, meaning that the catalytic reactions are much faster than the interconversion process between ES_1 and ES_2; (ii) $\beta \to 0$, meaning no interconversion between ES_1 and ES_2; (iii) $\alpha \to 0$, meaning no interconversion between E_1 and E_2; (iv) $(k_{21} + k_{-11})/k_{11} = (k_{22} + k_{-22})/k_{12}$, meaning the identical Michaelis constants in the two channels of $E_1 + S \leftrightarrow ES_1 \to {E_1}^0 + P$ and $E_2 + S \leftrightarrow ES_2 \to {E_2}^0 + P$; (v) $\alpha \to \infty$, meaning a fast interconversion between E_1 and E_2; and (vi) $k_{11} = k_{12}$ and $\beta \to \infty$, meaning the identical interconversion rate constant for the steps E_1 to ES_1 and E_2 to ES_2, and ultrafast interconversion between ES_1 and ES_2.

In some recent observation of slow conformational fluctuations, condition (i) mentioned above is usually not so stringent [17]. If the interconversion rate constant (α) between E_1 and E_2 is small, the dynamic disorder is quasi-static. In this case, there is a time lag between the fast catalytic reaction and the sluggish interconversion. Then, the steady-state waiting time distribution could be obtained in approximation

$$f(t) = \sum_{i=1}^{2} w_i \frac{k_{1i}k_{2i}[S]}{2A_i}[\exp(A_i + B_i)t - \exp(B_i - A_i)t] \tag{2.25}$$

where $A_i = \sqrt{(k_{1i}[S] + k_{-1i} + k_{2i})^2/4 - k_{1i}k_{2i}[S]}$, $B_i = -(k_{1i}[S] + k_{-1i} + k_{2i})/2$, and the weights W_1 and W_2 are

$$W_1 = \frac{k_{11}k_{21}(k_{22} + k_{-12})}{k_{11}k_{21}(k_{22} + k_{-12}) + k_{12}k_{22}(k_{21} + k_{-11})}$$
$$W_2 = \frac{k_{12}k_{22}(k_{21} + k_{-11})}{k_{11}k_{21}(k_{22} + k_{-12}) + k_{12}k_{22}(k_{21} + k_{-11})} \tag{2.26}$$

From Eq. (2.25), one can obtain the single molecule Michaelis–Menten equation for the two conformer cases:

$$\frac{1}{\langle t \rangle} = \frac{\chi_2'[S]}{[S] + C_M'} \tag{2.27}$$

where χ_2' is the weighted harmonic mean of the catalytic rate constants in the two channels and the apparent catalytic rate constant is

$$\frac{1}{\chi_2'} = \frac{w_1}{k_{21}} + \frac{w_2}{k_{22}} \tag{2.28a}$$

and C_M' is a complex function of the catalytic and Michaelis constants of the two conformers and the apparent Michaelis constant is

$$C_M' = \chi_2' \left[\frac{w_1 K_{M1}}{k_{21}} + \frac{w_2 K_{M2}}{k_{22}} \right] \tag{2.28b}$$

with $K_{Mi} \equiv (k_{-1i} + k_{2i})/k_{1i}$.

Equations (2.27) and (2.28a) indicate that single molecule Michaelis–Menten equation holds even in the presence of dynamic disorder, although the meanings or forms of χ_2' and C_M' are slightly different from that of k_2 and K_M in the classic Michaelis–Menten equation. In the following, it will further show that even a system with an arbitrary number of conformers also holds such form.

(ii) *Multistate model*: In reality, the real enzyme systems can usually interconvert among multiple conformational substrates. In this section, the two-state model introduced above is further generalized to a common model. In it, every enzyme species (E, ES, or E^0) in Eq. (2.1) can have any number (n) of mutually interconverting conformers, as indicated by the following kinetic scheme for the n-state Michaelis–Menten mechanism:

$$\begin{array}{ccccccc}
S + E_1 & \underset{k_{-11}}{\overset{k_{11}[S]}{\rightleftarrows}} & ES_1 & \xrightarrow{k_{21}} & P + E_1^0 & \xrightarrow{\delta_1} & E_1 \\
\alpha_{12}\downarrow\uparrow\alpha_{21} & & \beta_{12}\downarrow\uparrow\beta_{21} & & \gamma_{12}\downarrow\uparrow\gamma_{21} & & \\
S + E_2 & \underset{k_{-12}}{\overset{k_{12}[S]}{\rightleftarrows}} & ES_2 & \xrightarrow{k_{22}} & P + E_2^0 & \xrightarrow{\delta_2} & E_2 \\
\vdots & & \vdots & & \vdots & & \\
\downarrow\uparrow & & \downarrow\uparrow & & \downarrow\uparrow & & \\
\vdots & & \vdots & & \vdots & & \\
S + E_n & \underset{k_{-1n}}{\overset{k_{1n}[S]}{\rightleftarrows}} & ES_n & \xrightarrow{k_{2n}} & P + E_n^0 & \xrightarrow{\delta_n} & E_n
\end{array} \tag{2.29}$$

It should be noted here that E_i can interconvert with any other conformer not just with E_{i+1} or E_{i-1}, and the conformer ES_i does in the same way. The